THE JOURNAL OF PHYSICAL CHEMISTRY B

ARTICLE

pubs.acs.org/JPCB

Preference for Isolated Water Molecules in a Concentrated Glycerol−Water Mixture

J. J. Towey,[†] A. K. Soper,[‡] and L. Dougan*[,†]

[†]School of Physics and Astronomy, University of Leeds, Leeds, LS2 9JT, United Kingdom

[‡]ISIS Facility, Rutherford Appleton Laboratory, Chilton, Didcot, Oxon, OX11 OQX, United Kingdom

ABSTRACT: Neutron diffraction coupled with hydrogen/deuterium isotopic substitution has been used to investigate the structure of a concentrated glycerol water (4:1 mole fraction) solution. The neutron diffraction data were used to constrain a three-dimensional computational model that is experimentally relevant using the empirical potential structure refinement technique. From interrogation of this model, we find that glycerol−glycerol hydrogen bonding is largely unperturbed by the presence of water in the solution. We find that glycerol−water hydrogen bonding is prevalent, suggesting that water molecules effectively take the place of glycerol molecules in this concentrated solution. In contrast, we find that water−water hydrogen bonding is significantly perturbed. While the first coordination shell of water in the concentrated solution remains similar to that of pure water, water−water hydrogen bonding is greatly diminished beyond the first neighbor distance. Interestingly, the majority of water molecules exist as single monomers in the concentrated glycerol solution. The preference of isolated water molecules results in a solution that is well mixed with optimal glycerol−water hydrogen bonding. These results highlight the importance of preferential hydrogen bonding in aqueous solutions and suggest a mechanism for cryoprotection by which glycerol effectively hydrogen bonds with water, resulting in a disrupted hydrogen-bonded water network.

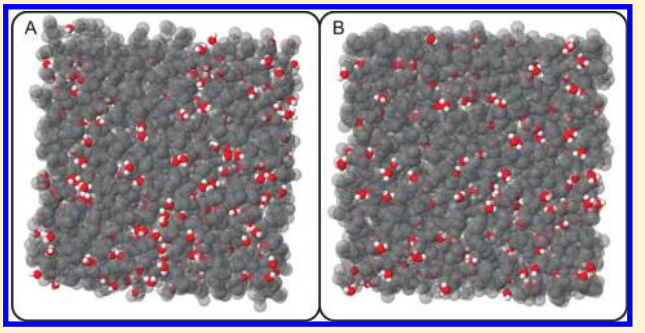

1. INTRODUCTION

Cryopreservation is an effective process in which molecules, cells, or whole tissues are preserved by cooling to subzero temperatures.[1−3] This method is widely utilized in nature, industry, medicine, and nanotechnology to prolong the storage life of specific components.[4−7] This important process is possible due to molecules called cryoprotectants, such as sugars and low molecular weight alcohols. The molecular mechanisms by which these cryoprotectants stabilize and protect molecules and cells, while suppressing the formation of ice, are incompletely understood.[6] Elucidating such molecular mechanisms is crucial to improve cryopreservation protocols as well as to identify and formulate more efficient cryoprotectant solutions.[8] One such cryoprotectant molecule is glycerol ($CH_2OHCHOHCH_2OH$), a sugar alcohol, which has been the subject of considerable scientific interest. The interest in glycerol has partly stemmed from its extensive use as a cryoprotectant and its glass-forming abilities.[9−12] The discovery of the cryoprotective properties of glycerol by Polge et al. in 1949 led to the development of artificial cryopreservation.[13,14] This early success led many investigators to attempt the preservation of other cells and tissues by similar empirical procedures.[15] In the present day, aqueous mixtures of glycerol are used to preserve the functionality of biological molecules during cooling and thawing processes, and to suppress intracellular ice formation, which can be harmful to cells and tissues.[16] However, a molecular-level understanding of the mechanisms that make glycerol a good cryoprotectant is still missing.[6] In particular, little is known about how glycerol affects water structure in order to suppress/favor crystallization or how concentration affects the cryoprotectant properties of glycerol solutions.[17] Knowledge of the structure of glycerol water mixtures may therefore help to develop better cryopreservation protocols and propose more optimal cooling and thawing regimes for cellular cryosolutions.[18,19]

In addition to their importance in industry and medicine, cryoprotectants are prevalent in nature in a wide range of organisms. Glycerol is a common cellular component and exists in algae, salt-tolerant plants, insects, fish, and reptiles that are exposed to cold temperatures.[20] In some instances, glycerol can be found in very high concentrations (>2 M), where it plays an important role in osmotic adaption and salt tolerance in environments of high salinity.[21,22] For example, studies have shown that glycerol is an important solute in the salt-loving, halophilic organism *Horatea weneckii*, a yeast that is a ubiquitous inhabitant of hypersaline waters.[23] While the occurrence of glycerol in nature has long been noted,[5,21] elucidating the molecular mechanisms by which glycerol molecules influence the stability of biological molecules has proven to be challenging.

Received: April 5, 2011
Revised: May 10, 2011
Published: May 25, 2011

dx.doi.org/10.1021/jp203140b | *J. Phys. Chem. B* 2011, 115, 7799–7807

Table 1. Glycerol−Water Samples for Which the Structure Factor Has Been Measured with Neutron Diffraction on the SANDALS Instrument[a]

sample no.	sample name	description
1	glycerol-D8 D_2O	fully deuterated glycerol (98 atom % D) with D_2O (purity 99.99% D)
2	glycerol-D5 H_2O	carbonyl atoms are deuterium and hydroxyl are hydrogen (98 atom % D) with Milli-Q water
3	glycerol-D5HD3 HDO	1:1 mixture of samples 1 and 2 with a 1:1 mixture of Milli-Q water and D_2O (purity 99.99% D)
4	glycerol-H8 H2O	fully protiated (99.5%) with Milli-Q water
5	glycerol-HD8 HDO	1:1 mixture of samples 1 and 4 with a 1:1 mixture of Milli-Q water and D_2O (purity 99.99% D)

[a] Deuterium oxide D_2O (99.5%), glycerol (99.5%), glycerol-d_3 (98 atom % D), and glycerol-d_8 (98 atom % D) were supplied by Sigma-Aldrich.

To try to understand how glycerol functions as a cryoprotectant, the physical properties of glycerol and its mixtures with water have been studied extensively by a number of simulations and experimental techniques. Kyrychenko et al.[24] completed molecular dynamics simulations to investigate the solubility behavior of cryoprotective solutes, such as glycerol, in pure water. This study suggested that, while some cryoprotectants, such as DMSO, mix rapidly with water so that all the solute molecules are distributed uniformly, for the glycerol−water system the solute molecules are not ideally mixed at the molecular level. The authors suggested that the mixing dynamics of the glycerol molecules in the surrounding water is strongly dependent on the nature of the hydrophilic and hydrophobic interactions between the glycerol molecules.[24] A recent study by Chen et al.[25] used molecular dynamics simulations to examine the hydrogen bonding network and dynamics of glycerol−water solutions ranging in concentration from 0.031 to 0.133 mole fraction glycerol. The authors proposed that as glycerol concentration increases, the hydrogen bonding "ability" of oxygen atoms in water decreases, leading to a decrease in the hydrogen bonding ability of water. The excess thermodynamic functions of glycerol−water mixtures have been calculated at room temperature using experimental data of vapor pressures, heats of mixing, and densities.[26] This work also calculated preferential solvation values across the concentration range and found that water−water interactions reach a maximum at around 0.25 mole fraction glycerol, while glycerol−water interactions reach a maximum at around 0.60 mole fraction glycerol. At a concentration of 0.75 mole fraction glycerol, water−glycerol interactions are preferred to water−water interactions.[26] Dashnau et al.[1] used molecular dynamics simulations and infrared spectroscopy to investigate the hydrogen bond patterns of glycerol and its mixtures with water. This study found that at glycerol concentrations above 0.50 mole fraction glycerol, most water molecules exist as monomers in the solution. Raman spectroscopy has been used to study glycerol/D_2O mixtures across the concentration range.[27] By analysis of specific peaks in the Raman spectrum, the authors concluded that at a concentration of 0.32 mole fraction glycerol, most D_2O molecules existed in the solution as monomers, forming hydrogen bonds with glycerol molecules rather than with other water molecules.

The variability of results produced using computer simulations and the lack of experimental data on the structure of glycerol−water solutions, mean that a systematic experimental investigation of the structure of these mixtures is required. In the present structural study, we have examined glycerol and water interactions and tested whether water molecules do indeed exist as monomers in a concentrated glycerol solution. Furthermore, we have determined whether isolated water molecules simply result from the constraints of low water concentration or if they are a consequence of the hydrogen bonding properties of this important cryoprotectant solution. In our experimental study, we provide a full atomistic-level, structural examination of a concentrated glycerol−water solution (0.80 mole fraction). We use experimental and computational methods to allow for the determination of a complete set of partial radial distribution functions (RDFs) of glycerol and water in the liquid state. Neutron diffraction is a suitable probe for the structural study of liquid glycerol due to the large scattering cross section of deuterium and the high contrast achievable using H/D selective substitution on specific hydrogen sites in the molecule. The main goal of this work was to obtain high-quality structural data of a concentrated glycerol−water solution and to investigate the hydrogen bonding interactions between glycerol and water molecules. This has been accomplished by supplementing the isotopic substitution neutron diffraction experiments with computer modeling. Specifically, the modeling is a three-dimensional molecular reconstruction using the empirical potential structure refinement (EPSR) method, which is constrained by experimental neutron diffraction data, described in the following section.

2. METHODS

2.1. Neutron Diffraction Experiments. Neutron diffraction coupled with isotopic substitution allows labeling of individual atomic sites in a molecule and the extraction of RDFs, $g(r)$. Neutron diffraction experiments were completed on the SANDALS time-of-flight diffractometer at the ISIS pulsed neutron facility at the Rutherford Appleton Laboratory, U.K. The instrument SANDALS is a total scattering neutron diffractometer optimized for the study of liquids and amorphous samples containing hydrogen. The physical quantity measured by the diffractometer is the differential scattering cross section $d\sigma/d\Omega$ as a function of the exchanged wave vector Q (defined as the difference between the incident and the scattered neutron wave vectors). Through the theory of neutron scattering,[12] it is possible to relate Q to the static structure factor $S(Q)$, which is the Fourier transform of the atomic pair distribution function $g(r)$. The function $g(r)$ provides information on how atomic densities vary as a function of radial distance, r, from any particular atom.[28]

Deuteriated samples of water and protiated and deuterated samples of anhydrous glycerol were obtained from Sigma-Aldrich and used without additional purification. Specifically, deuterated water (99.99% purity) was molecular biology grade, the protiated glycerol sample was molecular biology grade (≥99.5% purity), and deuterated glycerol (98% purity) and partially deuterated glycerol where the carbonyl atoms are deuterium while the hydroxyl are hydrogen (98%) were used. A total of five isotopically distinct samples were measured and are

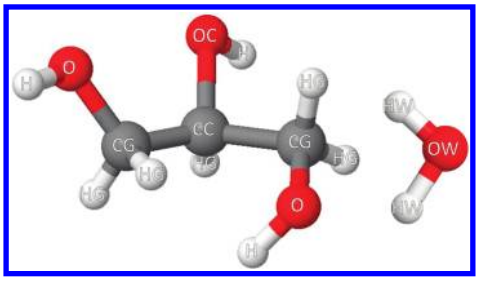

Figure 1. The glycerol and water molecules. The single atoms have been labeled according to the symbols used in the simulation and throughout this paper. For glycerol, the carbon atoms are labeled CG and CC, the oxygen atoms O and OC, the hydroxyl hydrogen atoms H, and the methyl hydrogen atoms HG. The water oxygen is labeled OW, and the water hydrogen is labeled HW.

shown in Table 1. These samples were placed in flat cells made from a titanium−zirconium alloy, which gives a negligible coherent scattering signal. These cells were mounted on an automated sample changer to cycle through the samples. The differential scattering cross-section for each sample was obtained by normalizing to a vanadium standard. Corrections for attenuation and multiple scattering were made using the ATLAS program suite, which has been detailed previously.[29] A further correction for inelastic scattering was made and has been described in detail elsewhere.[30] Neutron diffraction on solutions yields the quantity, $F(Q)$, which is the total interference differential scattering cross section, and which is the sum of all partial structure factors $S_{\alpha\beta}(Q)$ present in the sample, each weighted by their composition c and scattering intensity b, $F(Q) = \Sigma_{\alpha\beta} c_\alpha c_\beta b_\alpha b_\beta \, (S_{\alpha\beta}(Q) - 1)$, where Q is the magnitude of the change in momentum vector by the scattered neutrons ($Q = (4\pi/\lambda) \sin\theta$). Fourier transform of $S_{\alpha\beta}(Q)$ gives the respective atom−atom RDFs $g_{\alpha\beta}(r)$, and integration of $g_{\alpha\beta}(r)$ gives the coordination numbers of atoms α around atoms β between two distances r_1 and r_2.

2.2. Computational Modeling. In this paper we refer to two distinct atomic components in water and six distinct atomic components in glycerol molecules (see Figure 1). In the water molecule, the oxygen atom is labeled OW, while the hydrogen atom is labeled HW. In glycerol, the carbon atoms are labeled CC and CG and refer to the central and distal carbon atoms, respectively. The oxygen atoms are labeled OC and O, corresponding to the oxygen atoms attached to the central and distal carbon atoms, respectively. The hydrogen atoms are labeled H and HG for the hydroxyl and methyl hydrogen atoms, respectively. A full structural characterization of the system requires the determination of 36 RDFs, which is well beyond the capability of any existing diffraction technique by itself.

To build a model of glycerol and water liquid structure, the experimental data are used to constrain a computer simulation. In the simulation, the empirical potential is obtained directly from the diffraction data. This potential drives the structure of the three-dimensional model toward molecular configurations that are consistent with the measured partial structure factors from the neutron diffraction experiments. The diffraction data were interpreted via the EPSR computer simulation procedure.[29] EPSR aims to produce a model with a simulated differential scattering cross section ($Di(Q)$), which fits the experiment results as closely as possible. Given that in this case there are more site−site RDFs than diffraction data sets, extra information

Table 2. Geometry for Intramolecular Bonds within the Glycerol and Water Molecules Used in the EPSR Simulations[a]

intramolecular bond	length (Å)
O−CG	1.45
O−H	0.97
OC−H	0.97
OC−CC	1.45
CG−CC	1.54
CG−HG	1.08
CC−HG	1.08
OW−HW	1.00

[a] The geometry used for the glycerol molecules was optimized using the free computational chemistry software Ghemical 2.98. The water molecules have been produced using the SPC model.

Table 3. Geometry for Intramolecular Angles in Glycerol and Water Molecules Used in the EPSR Simulations[a]

intramolecular bond	angle (deg)
CG−O−H	109.90
CC−OC−H	108.33
O−CG−CC	108.88
CC−CG−HG	110.17
O−CG−HG	109.51
HG−CG−HG	108.57
CG−CC−CG	111.20
OC−CC−CG	108.72
CG−CC−HG	109.61
OC−CC−HG	108.96
HW−OW−HW	109.47

[a] The geometry for the glycerol molecules has been optimized using the free computational chemistry software Ghemical 2.98. The water molecules have been produced using the SPC model.

is required to define the structure. This is achieved by forcing the glycerol molecules in the simulation box to adopt the expected molecular geometries. A reference interaction potential is used which serves to generate hydrogen bonding between the relevant atom sites and to prevent atomic overlap at unrealistic distance ranges. The combined empirical and reference potentials do not guarantee that the final reconstruction of the structure is unique, but they do ensure that it is consistent with the diffraction data as well as being physically plausible.

For the simulations, a total of 948 glycerol molecules and 237 water molecules were contained in a cubic box of the appropriate dimension to give the measured density at 298 K. The intramolecular structure was optimized using the computational chemistry software Ghemical 2.98.[31] The intramolecular bond angles were taken from a previous study of pure glycerol.[32] This work used the conformer definitions of Bastiensen[33] to find that the $\alpha\beta$ structure showed the closest fit to the data.[32] The water molecules that were used were produced using the simple point charge (SPC) model.[34] A three-dimensional computer model of the solution is constructed and equilibrated using relevant interaction potentials (see Figure 1 for molecule conformation and Tables 2 and 3 for atomic geometry). The charges and Lennard-Jones constants are shown in Table 4. Periodic boundary conditions were imposed, and the Coulomb interactions are

Table 4. Lennard-Jones Parameters, Masses and Coulomb Charges Defining the Potentials Used for EPSR Simulations of Glycerol and Water at 298 K

atom name	ε (kJ/mol)	σ (Å)	m (a.m.u.)	q (e)
OC	0.65	3.100	16	−0.624
O	0.65	3.100	16	−0.624
CG	0.80	3.700	12	0.107
CC	0.80	3.700	12	0.170
H	0.00	0.000	2	0.392
HG	0.00	0.000	2	0.063
OW	0.65	3.166	16	−0.820
HW	0.00	0.000	2	0.410

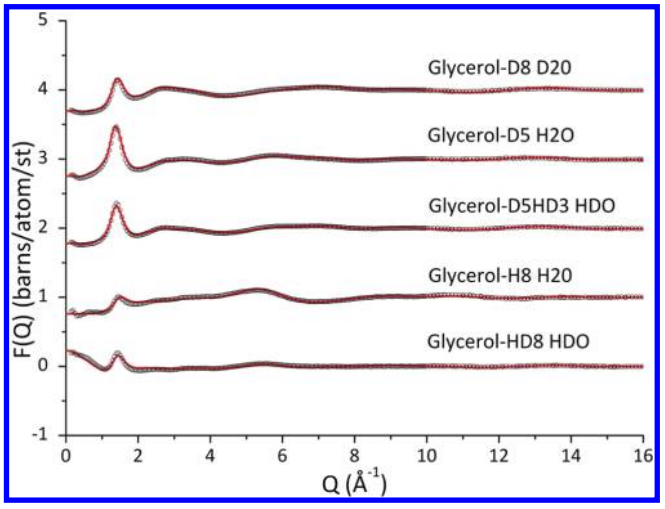

Figure 2. Fits (red lines) obtained by the EPSR analysis compared to the original data (black circles) for samples at a concentration of 4 glycerol molecules per water molecule (0.8 mole fraction glycerol) samples at 298 K. The data and fits are labeled according to Table 1 and have been shifted vertically for improved clarity. The data shown here confirm that this model produces a simulation that is in good agreement with the experimental data.

truncated by means of a derivative of the reaction field method,[35] and other interactions are truncated as described previously, using a radial cutoff of 12 Å in both cases.[36] Information from the diffraction data is then introduced as a constraint whereby the difference between observed and calculated partial structure factors enters as a perturbation potential to drive the computer model (via Monte Carlo updates of atomic positions) toward agreement with the measured data. The perturbation is refined in successive iterations of the procedure until a satisfactory fit is obtained. In this way an ensemble of three-dimensional molecular configurations of the mixture is generated, which exhibit average structural correlations that are consistent with the diffraction data.

3. RESULTS

The simulated and measured structure factors for the glycerol−water EPSR simulations can be compared in Figure 2. Here the $D_i(Q)$ obtained from the EPSR simulation (red lines) are compared to the neutron diffraction data $F_i(Q)$ (black circles) for glycerol and water at 298 K. In Figure 2, the $F_i(Q)$ plots have been labeled using the system shown in Table 1 and have been

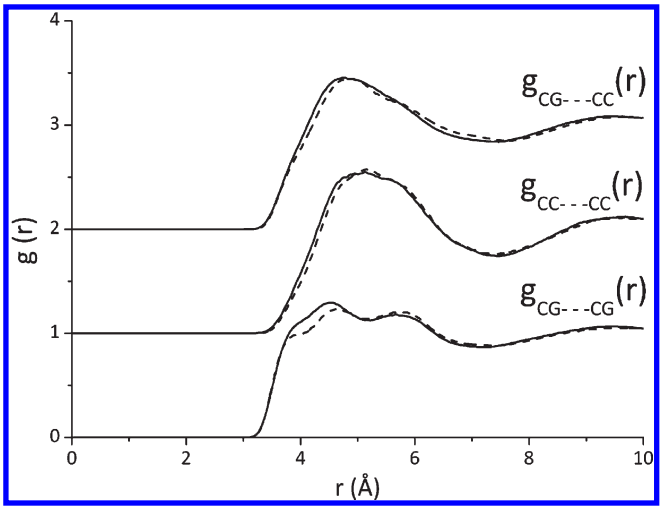

Figure 3. Glycerol−glycerol site−site partial RDFs for each of the three carbon−carbon pairings ($g_{CG\cdots CC}(r)$, $g_{CC\cdots CC}(r)$, and $g_{CG\cdots CG}(r)$) of the glycerol molecule. The RDFs are taken from the EPSR analysis of neutron diffraction data of a glycerol−water (4:1) mixture (dashed lines) and are compared with the same functions for pure glycerol from previously published data[32] (solid lines). The first peak positions have been shifted to larger values by 0.5−3.3%, indicating that the addition of water at 0.2 mole fraction has not had a dramatic effect on the structure of the carbon atoms within glycerol. These indicate that the structure of the glycerol molecules is not dramatically affected by the addition of water at this concentration.

shifted vertically for improved clarity. Minor discrepancies are observed in the low Q region and are caused by difficulties in removing the effect of nuclear recoil from the measured data. However, this recoil effect is expected to have a monotonic dependence on Q and so does not influence the model structure to any significant extent.

To begin our structural examination we investigated the pairwise distribution between glycerol molecules in the glycerol−water solution. Figure 3 shows the RDFs for carbon−carbon pairwise distributions, CG−CG, CC−CC, and CG−CC, in a glycerol−water (4:1) mixture (dashed lines) and the same function for pure glycerol (solid lines). The first peak positions in the glycerol−water mixture RDFs have shifted to slightly larger values by 0.5−3.3% in the concentrated glycerol−water mixture. Figure 4 shows the RDF for the methyl hydrogen−methyl hydrogen atoms of the glycerol molecule, HG−HG, for the glycerol−water (4:1) mixture (dashed lines). For comparison, we show the same function for pure glycerol (solid lines). The first peak position in Figure 4 is shifted to a shorter distance by around 3.5%, and the second peak is shifted outward by just over 2%. These minor changes in the RDF indicate that the addition of water has not had a dramatic effect on the structure of the methyl hydrogen atoms within glycerol at this concentration. Figure 5 shows the RDFs for oxygen−oxygen pairwise distributions, O−O, OC−OC, and O-OC, in a glycerol−water (4:1) mixture (dashed lines) and the same function for pure glycerol (solid lines). Comparison of the glycerol−water mixture and pure glycerol shows that the first peak positions of all glycerol oxygen−glycerol oxygen RDFs are unchanged (at ∼2.75 Å). The second peak positions of each RDF remain unchanged, indicating that the addition of water has not had a dramatic effect on the structure of the oxygen−oxygen interactions between glycerol molecules. All together, the RDFs in Figures 3−5

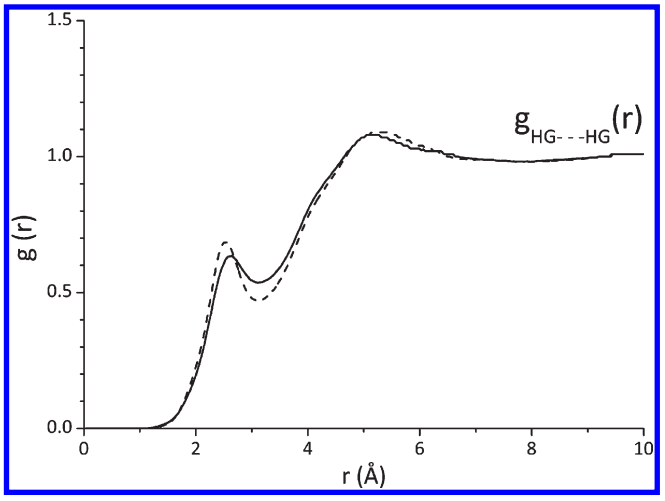

Figure 4. Glycerol−glycerol site−site partial RDFs for the methyl hydrogen−methyl hydrogen atoms ($g_{HG\cdots HG}(r)$) of the glycerol molecule. The RDFs are taken from the EPSR analysis of neutron diffraction data of a glycerol−water (4:1) mixture (dashed lines) and are compared with the same functions for pure glycerol from previously published data[32] (solid lines). The first peak position has been shifted to a shorter distance by around 3.5%, and the second peak is shifted outward by just over 2%, indicating that the addition of water has not had a dramatic effect on the structure of the methyl hydrogen atoms within glycerol at this concentration.

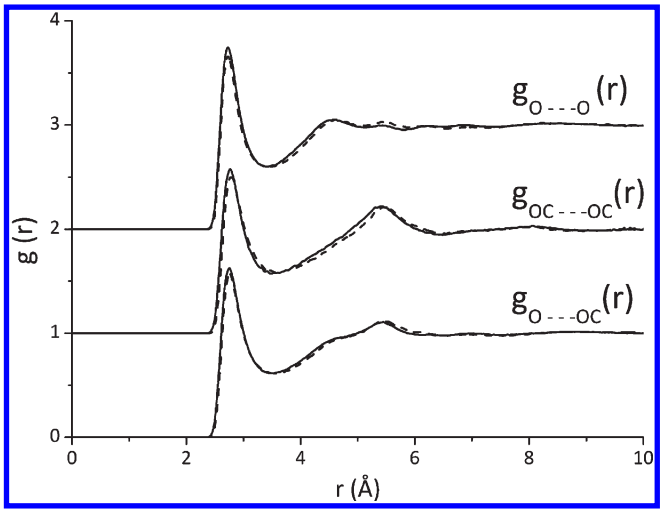

Figure 5. Glycerol−glycerol site−site partial RDFs for each of the three oxygen−oxygen pairings ($g_{O\cdots O}(r)$, $g_{OC\cdots OC}(r)$, and $g_{O\cdots OC}(r)$) of the glycerol molecule. The RDFs are taken from the EPSR analysis of neutron diffraction data of a glycerol−water (4:1) mixture (dashed lines) and are compared with the same functions for pure glycerol from previously published data[32] (solid lines). All of the first peak positions are unchanged (at ∼2.75 Å) for each of the distribution functions. The second peak positions of each RDF remain unchanged, indicating that the addition of water has not had a dramatic effect on the structure of the oxygen atoms within glycerol.

suggest that the local structure of glycerol−glycerol interactions is not greatly altered by the addition of water at this concentration. Glycerol is therefore capable of maintaining its structure despite the presence of 0.2 mole fraction of water molecules in the mixture.

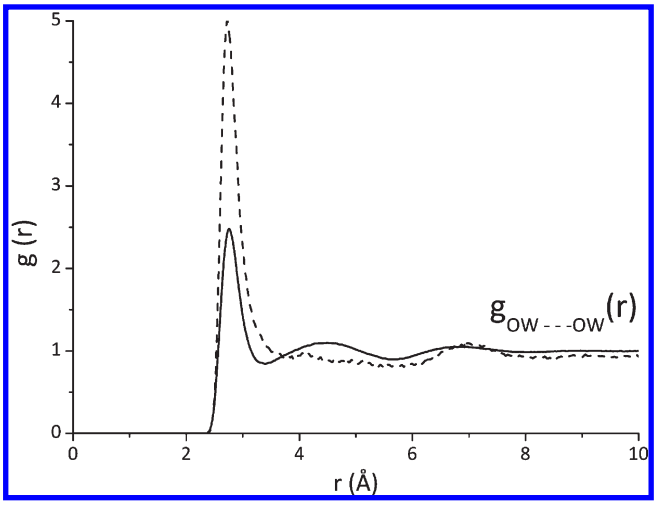

Figure 6. Water−water site−site partial RDFs for the oxygen−oxygen pairing ($g_{OW\cdots OW}(r)$) of the water molecule are shown. The RDFs are taken from the EPSR analysis of neutron diffraction data of a glycerol−water (4:1) mixture (dashed lines) and are compared with the same functions for pure water (solid lines). The pure water result has been produced using previously published pure data.[37]and the water molecular constraints used here (Tables 2−4). The first peak position is unchanged at ∼2.75 Å, but the peak height grows dramatically (roughly doubling). The second peak at ∼4.5 Å is not present in the glycerol−water mixture. This indicates that the tetrahedrality of the water is compromised in the presence of glycerol in this concentrated solution.

Next we examine the structure of water in this concentrated glycerol−water (4:1) mixture. Figure 6 shows the site−site partial RDFs for OW−OW in a glycerol−water (4:1) mixture (dashed line) and the same function for pure water (solid lines). The pure water result has been produced using previously published pure data[37]and the water molecular constraints used here (Tables 2−4). The first peak position of the OW−OW RDF is unchanged in comparison with pure water, at ∼2.75 Å, while the peak height grows dramatically (roughly doubling). Interestingly, no prominent second peak position is observed in the glycerol−water (4:1) mixture RDF, while water shows a distinctive peak at 4.5 Å.[37] This lack of order at the second neighbor level in the local structure suggests that the tetrahedrality of water−water structure is compromised by the presence of glycerol in this concentrated solution. Interestingly, a small peak in the glycerol−water mixture RDF is observed at around 7 Å.

RDFs provide more information than the average bond length given by the peak positions. The coordination number, the number of atoms of type β within certain distance parameters of a central atom of type α, can also be calculated. The coordination number ($n_{\alpha\beta}$) of atom type β around atom type α is given by

$$n_{\alpha\beta}(r) = 4\pi\rho c\beta \int_{r_1}^{r_2} r^2 g_{\alpha\beta}(r)\, dr$$

Where c_β is the number density of atom type β and ρ is the density of the system (atoms/Å). The first minimum in the relevant $g(r)$ is used for the maximum distance, r_2. The coordination number results are shown in Tables 5−7. Table 5 shows the coordination numbers based on the oxygen−hydrogen RDFs and is of particular interest as it can be used to calculate the number and type of hydrogen bonds present in the system. If we

Table 5. Coordination Numbers for Each of the Oxygen−Hydrogen Pair Correlation Functions within a 4:1 Glycerol:Water Mixture[a]

bond	r_1 (Å)	r_2 (Å)	1st peak position (Å)	coordination number	s.d.
O−H	0.00	2.52	1.77	0.86	0.63
O−HW	0.00	2.55	1.79	0.14	0.36
OC−H	0.00	2.55	1.83	0.90	0.64
OC−HW	0.00	2.31	1.80	0.11	0.32
OW−H	0.00	2.52	1.79	1.13	0.67
OW−HW	0.00	2.43	1.71	0.20	0.43

[a] The standard deviation (s.d.) has been calculated over 637 configurations for each of the coordination numbers.

Table 6. Coordination Numbers for the Oxygen−Oxygen Pair Correlation Functions within a 4:1 Glycerol:Water Mixture[a]

bond	r_1 (Å)	r_2 (Å)	1st peak position (Å)	coordination number	s.d.
O−O	2.28	3.50	2.73	1.56	0.91
O-OC	2.28	3.55	2.76	0.83	0.77
O-OW	2.28	3.55	2.76	0.34	0.56
OC-OC	2.28	3.60	2.76	0.85	0.78
OC-OW	2.28	3.70	2.76	0.36	0.58
OW-OW	2.28	3.80	2.76	0.63	0.83

[a] The standard deviation (s.d.) has been calculated over 637 configurations for each of the coordination numbers.

Table 7. Coordination Numbers for the Carbon−Carbon Pair Correlations Functions within a 4:1 Glycerol:Water Mixture[a]

bond	r_1 (Å)	r_2 (Å)	1st peak position (Å)	coordination number	s.d.
CG−CG	3.00	5.18	4.65	6.94	1.53
CG−CG	3.00	7.31	5.72	23.73	2.11
CG−CC	3.00	7.66	4.77	13.63	1.51
CC−CC	3.00	7.46	5.13	12.74	1.42

[a] The standard deviation (s.d.) has been calculated over 637 configurations for each of the coordination numbers.

first consider the glycerol−glycerol hydrogen bonding, we find that there are 0.90 OC···H hydrogen bonds and 1.71 (2 × 0.86) O···H hydrogen bonds per molecule. This symmetrically means that there are 0.90 H···O and 1.72 H···O hydrogen bonds per molecule. Therefore, there is a total of 5.23 ± 1.51 glycerol−glycerol hydrogen bonds. Glycerol can also form hydrogen bonds to water molecules either as a donor (OW···H) or acceptor (O···HW or OC···HW). The OW···H value quoted in Table 5 is the number of OW···H bonds per water oxygen. As there are 4 times the amount of glycerol molecules compared to water molecules, this number (1.22) must be divided by 4 to provide the number of these bonds per glycerol molecule (0.30). The glycerol acceptor values also need to be corrected to provide the amount of bonds per molecule. This gives a value of 0.40 glycerol oxygen−water hydrogen bonds per glycerol molecule.

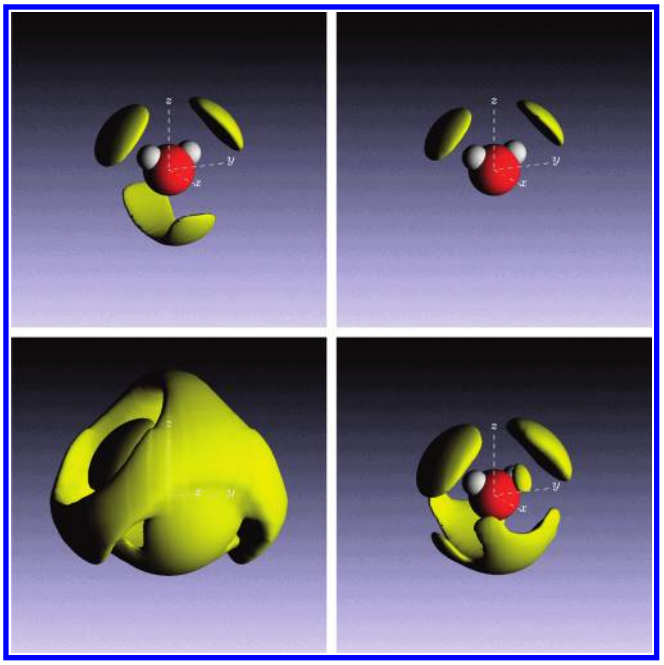

Figure 7. SDFs for the water oxygen atoms found around a central water molecule. The SDFs are taken from the EPSR analysis of neutron diffraction data of a glycerol−water (4:1) mixture (right) and are compared with the same functions for pure water (left). The pure water result has been produced using previously published pure data[37] and the water molecular constraints used here (Tables 2−4). The yellow shaded areas represent the regions where the probability of finding another water molecule within 5.7 Å of the central oxygen atom exceeds 7% (top) and 25% (bottom).

Therefore the total number of glycerol−water hydrogen bonds is 0.70 ± 0.95. Combining these values gives a total number of hydrogen bonds per glycerol molecule of 5.94 ± 1.57. This is very similar to the value taken from a previous investigation of pure glycerol,[32] which found that there were 5.68 ± 1.51 hydrogen bonds per glycerol molecule. This is further evidence that the hydrogen bond network of glycerol is not perturbed by the addition of water at a concentration of 0.2 mole fraction.

A similar analysis has been used to calculate the number of hydrogen bonds per water molecule. The number of water−water hydrogen bonds was 0.40 ± 0.93 and water···glycerol hydrogen bonds was 2.81 ± 1.36 leading to a total number of hydrogen bonds per water molecule of 3.21 ± 1.51. This is similar to the value calculated using previously published water data[37] 3.56 ± 1.10. This suggests that water−glycerol hydrogen bonding compensates for the decrease in water−water hydrogen bonding in this system.

To further investigate the three-dimensional structure of water in this mixture, it is instructive to use the RDFs to produce a three-dimensional analogue, the spatial density function (SDF). This is done by fixing the orientation of a central molecule and using this as the basis for a coordinate system. The number of molecules that surround this central molecule can be calculated as a function of radial distance, azimuthal angle, and elevation angle. This is repeated for all the relevant molecules and for an ensemble of configurations. In Figure 7 we show the SDFs for water oxygen atoms found around a central water molecule. The SDFs are taken from the EPSR analysis of neutron diffraction data of glycerol−water (4:1) mixture (right) and are compared with the same functions for pure water (left). The pure water

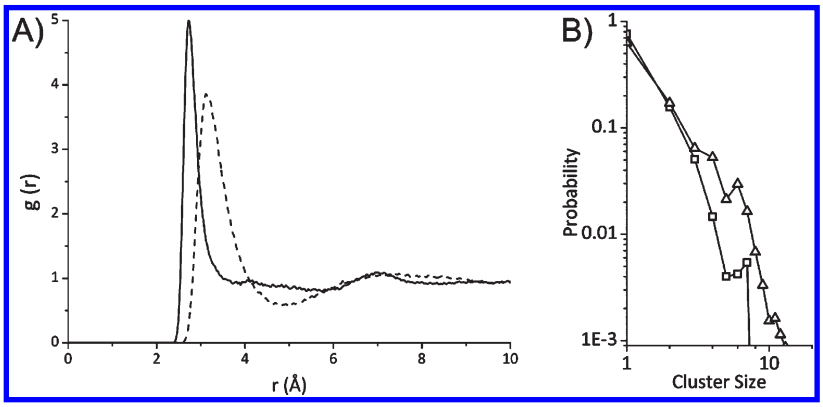

Figure 8. (A) OW−OW site−site partial RDFs. The RDFs are taken from the EPSR analysis of neutron diffraction data of a glycerol−water (4:1) mixture (solid line) and are compared with the same function taken from a simulation where all columbic and empirical potentials have been removed (dotted line). The r_{max} values used for the cluster analysis are taken from the positions of the first minima in each RDF: 3.80 Å for the EPSR data and 4.89 Å for the simulation without Coulombic or empirical potentials. (B) Cluster size distributions for glycerol−water solutions. The results taken from EPSR are shown with squares, and the results from the simulation without Columbic or empirical potentials are shown with triangles. From this it was found that most of the water molecules (55.7%) are found as monomers within the EPSR analysis with the largest clusters consisting of 7 water molecules. If this were an effect due to the packing of the molecules, then a similar result would be found when the Columbic and empirical potentials have been removed. The result found using this system was that around one-third (32.8%) of the molecules were monomers with the largest clusters consisting of 16 molecules.

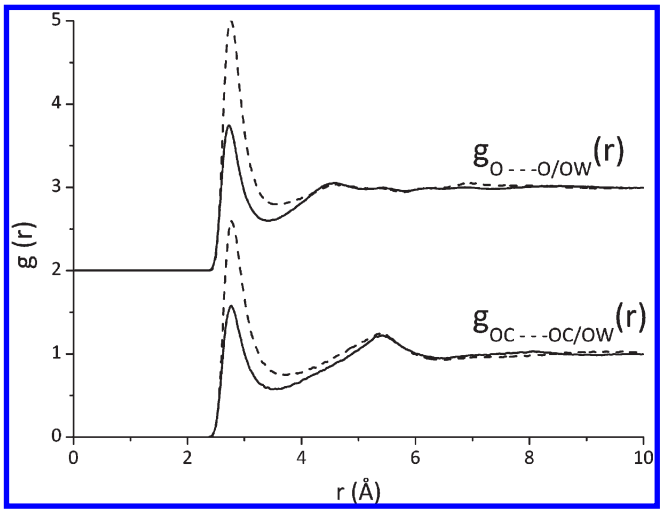

Figure 9. Glycerol−water site−site partial RDFs for each of the two glycerol oxygen−water oxygen pairings ($g_{O\cdots OW}(r)$, $g_{OC\cdots OW}(r)$). The RDFs are taken from the EPSR analysis of the neutron diffraction data of a glycerol−water (4:1) mixture (dashed lines) and are compared with the glycerol oxygen−glycerol oxygen functions ($g_{O\cdots O}(r)$, $g_{OC\cdots OC}(r)$) for pure glycerol from previously published data[32] (solid lines). It can be seen that the positions of the first and second peaks in the water oxygen−glycerol oxygen RDFs do not differ compared to the glycerol oxygen−glycerol oxygen RDFs taken from previously published pure glycerol data. This suggests that the addition of the water molecules does not disrupt the structure of the hydrogen bond network of glycerol.

result has been produced using previously published pure data[37] and the water molecular constraints used here (Tables 2−4). The yellow areas represent regions of high water density around a central water molecule. In the case of pure water (Figure 7, left) the familiar tetrahedral first coordination shell can be seen (top), this is then followed by a well-defined second shell (bottom). The result taken from the glycerol−water data does not show this well-defined structure (Figure 7, right). This is further evidence for the disruption of the tetrahedrality of water in the presence of glycerol at this concentration.

We examine the details of water clusters by calculating the cluster size distribution, which is the probability of finding a cluster of a particular size as a function of cluster size. The EPSR-generated ensembles were interrogated to extract structural information on water clusters in the solution. The water clusters are defined by those molecules that participate in a continuous hydrogen bonded network. Two water molecules are considered to be hydrogen bonded if the interoxygen contact distance is less than the radial distance of the first minimum of the $g_{OwOw}(r)$ (Figure 8a). Figure 8b shows the number of clusters containing i water molecules as a fraction of the total number of clusters $M(i)/M$ [where $M = \Sigma_i M(i)$] against cluster size i. Here, the data extracted from the EPSR simulation (squares) is compared to that taken from a simulation where the Coulombic and empirical potentials have been removed (triangles). Any clustering/segregation found in the results taken from the simulation without Coulombic or empirical potentials can be ascribed to an effect purely due to molecular packing.

Figure 8b shows that most of the water molecules (55.7%) exist as monomers in a concentrated glycerol−water (4:1) mixture (squares). The largest clusters were found to consist of seven water molecules. The cluster size distribution for the system where Coulombic and empirical potentials have been removed (triangles) shows that only a third (32.8%) of the water molecules exist as monomers in the solution, with the majority of water molecules existing in clusters of size two or more, with a maximum cluster size of 16 water molecules. This shows that the monomers shown within the EPSR simulation are not due to a packing effect. The lack of water clustering suggests that water−glycerol interactions are more favorable than water−water interactions at this concentration. This results in a solution that has a large number of isolated water molecules that are bonded to the surrounding glycerol molecules.

To examine this further we consider the hydrogen bonding between glycerol and water molecules by examining the glycerol oxygen−water oxygen site−site partial RDFs, O−OW and

dx.doi.org/10.1021/jp203140b |J. Phys. Chem. B 2011, 115, 7799–7807

OC−OW. In Figure 9, the RDFs for O−OW and OC−OW for a glycerol−water (4:1) mixture (dashed lines) are shown, as well as the same glycerol oxygen−glycerol oxygen functions ($g_{O\cdots O}(r)$, $g_{OC\cdots OC}(r)$) for pure glycerol. It can be seen that the RDFs are very similar for the glycerol−water solution and pure glycerol, suggesting that water molecules readily replace glycerol molecules in the glycerol hydrogen bond network.

4. DISCUSSION

In this study we have examined the hydrogen bonding of glycerol and water in a concentrated (4:1) mixture. This has been achieved by a combination of neutron diffraction with isotopic substitution and EPSR modeling. The models that have been produced for glycerol and water are consistent with the experimental results and provide new insight into the structural properties of an important cryoprotectant molecule. We find that glycerol−glycerol interactions maintain a similar structure to that found in pure glycerol, despite the presence of 0.2 mole fraction of water molecules in the mixture. This suggests that glycerol is unperturbed by the presence of water molecules at this concentration and is effective at maintaining its hydrogen bonded network. Interestingly, we find that glycerol−water hydrogen bonding is also prominent in this concentrated solution, suggesting that water molecules effectively take the place of glycerol molecules. In contrast to the prominence of glycerol−glycerol and glycerol−water interactions, we find that water−water interactions are greatly perturbed in this concentrated glycerol solution. While the first coordination shell of water in the concentrated solution remains similar to that of pure water, we find water−water hydrogen bonding is greatly diminished beyond first neighbor distance. We find that a disruption of the water−water interactions results from the dominance of isolated water molecules in the solution. These preferred, isolated water molecules come at the expense of water clusters in the solution. This is in agreement with previous work,[1] which found that at glycerol concentrations above 0.50 mole fraction glycerol, most water molecules existed as monomers in the solution. The results are also in agreement with previous Raman spectroscopy results,[27] which suggested that at a concentration of 0.32 mole fraction glycerol, most water (D_2O) molecules existed in the solution as monomers, preferring to form hydrogen bonds with glycerol molecules rather with themselves. Furthermore, calculation of preferential solvation values across the concentration range found that at a concentration of 0.75 mole fraction glycerol, glycerol−water interactions are preferred to water−water interactions.[27] Therefore the conclusion of our work appears to be in agreement with previous studies, which use a range of experimental and computational approaches. Importantly, our results provide the first structural measurement of this system and suggest that water molecules have a preference to exist as isolated monomers in a concentrated glycerol solution. Furthermore, we have demonstrated that the prevalence of isolated water molecules in the solution is more than would be expected from simple concentration and packing effects alone.

Given glycerol's role as a cryoprotectant molecule, it is interesting to compare the structural properties of glycerol, a sugar alcohol, with that of methanol, an alcohol. A cluster analysis of the distribution of water molecules (Figure 8), derived from the EPSR simulation of the experimental data, provides structural insight into water clusters in the solution. If water and the alcohol or sugar alcohol were randomly mixed at the molecular level, most water would exist as isolated molecules in concentrated solutions, with distinct water clusters being rare. Previous work has shown that methanol−water mixtures microsegregate to form water-rich and methanol-rich clusters.[38−40] This work showed that in a concentrated methanol−water (7:3) mixture, water molecules exist as clusters in a fluid of close-packed methyl groups, with water clusters bridging neighboring methanol hydroxyl groups through hydrogen bonding. Furthermore, although single water molecules exist (cluster size 1), these constitute only 13% of all water molecules in the mixture. The remaining 87% water molecules occur in clusters containing 2−20 or more molecules. Conversely, in the concentrated glycerol−water (4:1) mixture in the present study, we find that the majority of water molecules exist as isolated monomers (55.7%). This preference for isolated water molecules is more than just a simple packing effect where we might expect around 32.8% of isolated water molecules. Therefore, in a concentrated glycerol−water solution, there seems to be a preference for isolated water molecules that goes beyond that expected for the mixture. Given the presence of unperturbed glycerol−glycerol interactions and lack of water clusters, it is interesting to consider the role played by glycerol in preventing ice formation. We find that glycerol and water molecules mix very effectively, hindering the formation of an extended water network in the solution and hence the formation of ice. Furthermore, given the efficiency of water molecules to take the place of glycerol molecules in the hydrogen bonded network, an extended glycerol network is impeded. Thus, we propose that it is the good mixing of this solution and the preference of water monomers that prevent water networks from penetrating and perhaps disrupting biological systems. Given glycerol can be found in high concentrations in biological systems,[21,22] the mixing of aqueous glycerol and preference for water monomers could offer an attractive structural mechanism for protecting organisms under extreme cold conditions. Further studies on a dilute and intermediate concentration of glycerol solutions will help to elucidate whether this structural picture is valid across the concentration regime.

AUTHOR INFORMATION

Corresponding Author
*E-mail: L.Dougan@leeds.ac.uk.

ACKNOWLEDGMENT

This work was supported by a grant to L.D. from the Engineering Physics Science Research Council (EPSRC), UK (grant EP/H020616/1), and through an EPSRC funded DTA studentship to J.J.T. Experiments at the ISIS Pulsed Neutron and Muon Source were supported by a beamtime allocation from the Science and Technology Facilities Council. We are grateful to Dr. Silvia Imberti and Dr. Rowan Hargreaves at the ISIS Facility, Rutherford Appleton Laboratory, for their support.

REFERENCES

(1) Dashnau, J. L.; Nucci, N. V.; Sharp, K. A.; Vanderkooi, J. M. *J. Phys. Chem. B* **2006**, *110*, 13670.
(2) Gekko, K.; Timasheff, S. N. *Biochemistry* **1981**, *20*, 4667.
(3) Yancey, P. H.; Clark, M. E.; Hand, S. C.; Bowlus, R. D.; Somero, G. N. *Science* **1982**, *217*, 1214.
(4) Miller, K. *Comp. Biochem. Physiol., Part A: Physiol.* **1982**, *73*, 595.
(5) Raymond, J. A. *J. Exp. Zool.* **1992**, *262*, 347.

(6) Zachariassen, K. E.; Kristiansen, E. *Cryobiology* **2000**, *41*, 257.
(7) Zachariassen, K. E.; Kristiansen, E.; Pedersen, S. A.; Hammel, H. T. *Cryobiology* **2004**, *48*, 309.
(8) Lynch, A. L.; Chen, R. J.; Dominowski, P. J.; Shalaev, E. Y.; Yancey, R. J.; Slater, N. K. H. *Biomaterials* **2010**, *31*, 6096.
(9) Dawidowski, J.; Bermejo, F. J.; Fayos, R.; Perea, R. F.; Bennington, S. M.; Criado, A. *Phys. Rev. E* **1996**, *53*, 5079.
(10) Doss, A.; Paluch, M.; Sillescu, H.; Hinze, G. *Phys. Rev. Lett.* **2002**, *88*, 095701.
(11) Doss, A.; Paluch, M.; Sillescu, H.; Hinze, G. *J. Chem. Phys.* **2002**, *117*, 6582.
(12) Fisher, H. E.; Barnes, A. C.; Salmon, P. S. *Rep. Prog. Phys.* **2006**, *69*, 233.
(13) Polge, C.; Smith, A. U.; Parkes, A. S. *Nature* **1949**, *164*, 666.
(14) Smith, A. U.; Polge, C. *Nature* **1950**, *166*, 668.
(15) Mironesc., S; Seed, T.; Meryman, H. *J. Cell Biol.* **1974**, *63*, A229.
(16) Mazur, P. *Science* **1970**, *168*, 939.
(17) Franks, F. *Biophys. Chem.* **2003**, *105*, 251.
(18) Chen, R. J.; Slater, N. K. H.; Gatlin, L. A.; Kramer, T.; Shalaev, E. Y. *Pharm. Dev. Technol.* **2008**, *13*, 367.
(19) Meryman, H. T. *Annu. Rev. Biophys. Bioeng.* **1974**, *3*, 341.
(20) Brown, A. D.; Simpson, J. R. *J. Gen. Microbiol.* **1972**, *72*, 589.
(21) Benamotz, A.; Avron, M. *Plant Physiol.* **1973**, *51*, 875.
(22) Kogej, T.; Stein, M.; Volkmann, M.; Gorbushina, A. G.; Galinski, E. A.; Gunde-Cimerman, N. *Microbiology* **2007**, *153*, 4261.
(23) Cantrell, S. A.; Casillas-Martinez, L.; Molina, M. *Mycol. Res.* **2006**, *110*, 962.
(24) Kyrychenko, A.; Dyubko, T. S. *Biophys. Chem.* **2008**, *136*, 23.
(25) Chen, C.; Li, W. Z.; Song, Y. C.; Yang, J. *J. Mol. Liq.* **2009**, *146*, 23.
(26) Marcus, Y. *Phys. Chem. Chem. Phys.* **2000**, *2*, 4891.
(27) Mudalige, A.; Pemberton, J. E. *Vib. Spectrosc.* **2007**, *45*, 27.
(28) Keen, D. A. *J. Appl. Crystallogr.* **2001**, *34*, 172.
(29) Soper, A. K. *Phys. Rev. B* **2005**, *72*, 104204.
(30) Soper, A. K. *Mol. Phys.* **2009**, *107*, 1667.
(31) Hassinen, T.; Perakyla, M. *J. Comput. Chem.* **2001**, *22*, 1229.
(32) Towey, J. J.; Soper, A. K.; Dougan, L. *Phys. Chem. Chem. Phys.* **2011**, *12*, 9397.
(33) Bastiansen, O. *Acta Chem. Scand.* **1949**, *3*, 415.
(34) Berendsen, H. J. C.; Grigera, J. R.; Straatsma, T. P. *J. Phys. Chem.* **1987**, *91*, 6269.
(35) Hummer, G.; Soumpasis, D. M.; Neumann, M. *J. Phys.: Condens. Matter* **1994**, *6*, A141.
(36) Soper, A. K. *Chem. Phys.* **1996**, *202*, 295.
(37) Soper, A. K. *J. Phys.: Condens. Matter* **2007**, *19*, 335206.
(38) Dixit, S.; Soper, A. K.; Finney, J. L.; Crain, J. *Europhys. Lett.* **2002**, *59*, 377.
(39) Dougan, L.; Bates, S. P.; Hargreaves, R.; Fox, J. P.; Crain, J.; Finney, J. L.; Reat, V.; Soper, A. K. *J. Chem. Phys.* **2004**, *121*, 6456.
(40) Dougan, L.; Hargreaves, R.; Bates, S. P.; Finney, J. L.; Reat, V.; Soper, A. K.; Crain, J. *J. Chem. Phys.* **2005**, *122*, 174514.